NANOSYSTEMS: PHYSICS, CHEMISTRY, MATHEMATICS, 2017, 8 (3), P. 371–377

Phase composition and magnetic properties of $Ni_{1-x}Co_xFe_2O_4$ nanocrystals with spinel structure, synthesized by Co-precipiation

Anh Tien Nguyen[1], Tien Dat Nguyen[1], V. O. Mittova[2], M. V. Berezhnaya[3], I. Ya. Mittova[3]
[1]Ho Chi Minh City Pedagogical University, Ho Chi Minh City, Vietnam
[2]Burdenko Voronezh State Medical University, Voronezh 394036, Russia
[3]Voronezh State University, Voronezh 394018, Russia
anhtienhcmup@gmail.com, tiendatpn@gmail.com, vmittova@mail.ru,
cnurova2010@yandex.ru, imittova@mail.ru

PACS 75.50.Cc, 81.07.Wx **DOI 10.17586/2220-8054-2017-8-3-371-377**

Nanopowders of nickel ferrite doped with cobalt were synthesized by co-precipitation using a 3 % KOH solution as a precipitant. The effects of different annealing regimes on the composition and particle size of $Ni_{1-x}Co_xFe_2O_4$ were studied. It was established that with annealing at $t = 1000$ °C for 2 h single-phase products were formed with a crystallite size of 30–50 nm. The saturation magnetization and the coercive force increased as the content of the dopant increased from 50.3 emu/g and 51.94 Oe for $NiFe_2O_4$ to 80.45 emu/g and 848.32 Oe for $CoFe_2O_4$.

Keywords: ferrites, spinel, nanocrystals, co-precipitation, magnetic properties.

Received: 7 April 2017

Revised: 12 May 2017

1. Introduction

Among magnetic materials, nanocrystalline ferrites with a spinel structure of type MFe_2O_4 (M = Co, Ni, Zn, Mn) are distinguished by high permeability, saturation magnetization and are used to produce new multifunctional materials, such as high-frequency devices, due to the decreased Foucault currents and increased duration of their functioning [1–5]. In addition, ferrites with a spinel structure are cheaper and more stable (in terms of time and temperature) compared to metals and alloys.

The magnetic and electrical characteristics of these ferrites depend on their chemical composition, cation location, particle size, dopant content and the synthesis method [1–9]. $CoFe_2O_4$ is hard magnetic ferrite with a high coercive force $H_c > 1500$ Oe, with an average saturation magnetization of $M_s \sim 40$ emu/g [10]. $NiFe_2O_4$ is a soft magnetic material characterized by small values of coercive force, saturation magnetization and excessive magnetization (H_c = 46.46 Oe, M_s = 8.8 emu/g, M_r = 0.2 emu/g) [1–3]. Different magnetic properties of ferrites are required for different applications and can be achieved in several ways: either by controlling the particle size, or by changing the concentrations of hard and soft magnetic phases in the material by introduction of another element (dopant) or by the formation of coatings on SiO_2 [11–14].

Sol-gel processes, including the formation of complexes with the addition of surfactants are promising for the synthesis of ferromagnetic oxide nanomaterials MFe_2O_4 (M = Co, Ni). An important advantage of such complexes is the lower annealing temperature in comparison to solid-phase synthesis, leading to decreased size of the obtained particles [2–5, 10, 11]. However, the formation of a single-phase product synthesized by the sol-gel method is affected by many factors, such as the annealing temperature and time, the gel formation temperature, the stoichiometry of the surfactant/metal ions, pH value, and others.

In previous studies [1, 12], MFe_2O_4 nanocrystals (M = Co, Ni) were obtained by co-precipitation of M^{2+} and Fe^{3+} cations at room temperature with the addition of an aqueous ammonia at pH = 11. However, at pH = 11, $Co(OH)_2$ and $Ni(OH)_2$ are dissolved with the formation of complexes with ammonia in accordance with the following equation:

$$M(OH)_2 \downarrow + 6NH_3 \rightarrow [M(NH_3)_6](OH)_2,$$

therefore, it is impossible to completely precipitate cobalt and nickel hydroxides with an aqueous solution of ammonia, which makes the achievement of the molar ratio $M^{2+} : Fe^{3+} = 1 : 2$ in the composition of precipitation complicated.

In this study, we investigated conditions for the formation of nanocrystals with the spinel structure $Ni_{1-x}Co_xFe_2O_4$ (x = 0; 0.2; 0.4; 0.6; 0.8; 1) by co-precipitation during the hydrolysis of M(II) and Fe(III) cations in boiling water, followed by cooling and addition of 3% aqueous KOH as a precipitant, as well as the phase composition and magnetic properties of the formed compounds. Hydrolysis of M(II) and Fe(III) cations in boiling water leads to the formation of a stable precipitate and decreased particle size compared to co-precipitation of the hydroxide ions at room temperature. Some nanosystems of $LnFeO_3$ (Ln = La, Y) type were obtained by this co-precipitation method [15, 16].

2. Materials and methods

2.1. Initial substances

The precursors for these syntheses were aqueous solutions of nickel (II), cobalt (II) and iron (III) nitrates (all – chemically pure) with a molar ratio of $Ni^{2+} : Co^{2+} : Fe^{3+} = (1 - x) : x : 2$. The precipitant was an aqueous solution of potassium hydroxide (3 %).

2.2. The synthesis of $Ni_{1-x}Co_xFe_2O_4$ nanoparticles

$Ni_{1-x}Co_xFe_2O_4$ nanoparticles were synthesized by adding 50 mL of a mixture containing $Ni(NO_3)_2$ 0.1 M, $Co(NO_3)_2$ 0.1 M and $Fe(NO_3)_3$ 0.2 M into 500 mL of boiling water with magnetic stirring. The obtained colloidal system was cooled to room temperature. The system acquired a reddish-brown color which it retained upon cooling. Then, 3 % aqueous solution of potassium hydroxide in the amount required for complete precipitation of the cations (until the disappearance of the phenolphthalein color) was added with magnetic stirring.

The precipitated hydroxides were stirred for 30–40 min with magnetic stirring. The obtained precipitate was separated using a vacuum filter, washed several times with distilled water and dried at room temperature to a constant weight.

2.3. Methods of investigation

The obtained samples were finely ground into a powder and subjected to complex thermal analysis using thermal analyzer Labsys Evo (TG-DSC 1600 °C, France), including thermogravimetric analysis (TGA) and differential-scanning calorimetry (DSC). The thermal analysis was carried out in the dry air. The heating rate was 10 °/min; the maximum heating temperature was 1100 °C.

The phase compositions of the samples were determined by X-ray phase analysis (XPA, diffractometer SIEMEN D – 5000 Brucker, Germany), CuK_α-radiation, $\lambda = 0.15406$ nm, $2\theta = 10$–80 °, measurement interval 0.02 °/sec. The obtained diffractograms were analyzed using the JCPDS database.

The average crystal size according to XPA data and the constant parameter of the spinel cubic lattice $Ni_{1-x}Co_xFe_2O_4$ were calculated by following equations:

$$d = \frac{0.89 \cdot \lambda}{\beta \cos\theta}, \tag{1}$$

$$a = \frac{\lambda}{2\sin\theta}\sqrt{h^2 + k^2 + l^2}, \tag{2}$$

where d – average crystal size, Å; λ – X-ray tube wavelength (for the copper tube used in this recording, $\lambda = 0.15406$ nm); 2θ – is the position of the maximum of the peak, deg; β – is the true physical broadening of the diffraction maximum, rad.; h, k, l – Miller indices, correspond to the peaks with the highest intensity.

The sizes and morphologies of the nanoparticles were determined by transmission electron microscopy (TEM–JEOL 1400, Japan).

Magnetic characteristics of $Ni_{1-x}Co_xFe_2O_4$ nanopowders were studied using a Microsene EV11 (Japan) vibration magnetometer at room temperature.

2.4. Results and discussion

The results of complex thermal analysis of the obtained precipitate for $Ni_{0.6}Co_{0.4}Fe_2O_4$ nanopowder before annealing, shown in Fig. 1, demonstrated that mass loss of the sample during all heat treatment processes from room temperature to 1100 °C was 16.61 % (TGA curve). The mass loss of the sample heated from 65 °C to 320 °C occurs rapidly, as indicated by the slope of TGA curve. Two peaks of endothelial effects at 200 °C and 27 °C, characteristic for desorption, evaporation and decomposition of nickel (II), cobalt (II) and iron (III) hydroxides were detected on DSC curve.

After that, the mass loss of the sample is slower, terminating at $\sim$ 650 °C due to the continuation of decomposition of hydroxides with formation of NiO, CoO and Fe_2O_3. At this point, a large peak corresponding to heat release at 500–650 °C appeared.

Subsequently, in accordance with the thermal analysis data of $Ni_{0.6}Co_{0.4}Fe_2O_4$, thermal treatment was carried out at 700, 800 and 1000°C for 2 h in order to establish the conditions for the formation of single-phase $Ni_{1-x}Co_xFe_2O_4$ products.

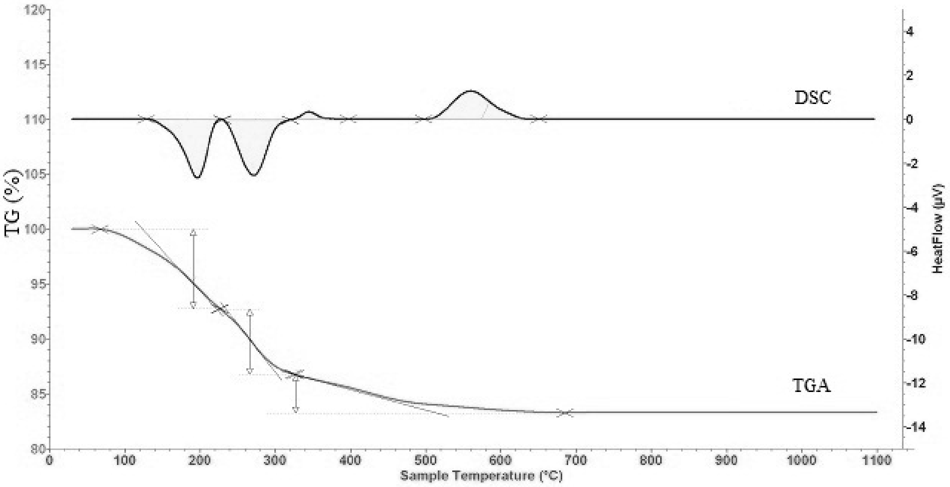

FIG. 1. DSC and TGA curves of precipitate sample for production of $Ni_{0.6}Co_{0.4}Fe_2O_4$ before annealing

The diffractograms of undoped $NiFe_2O_4$ (Fig. 2) after annealing at 700, 800 and 1000 °C showed that the background of lines of diffractograms are stable, the intensities of the peaks increase and their widths decrease at higher temperatures. Consequently, when the annealing temperature increased from 700 °C to 1000 °C, the degree of crystallization of the samples increased with decreasing average crystal size. The presence of only one phase of $NiFe_2O_4$ spinel with a cubic structure belonging to Fd3m spatial group (JCPDS 00-010-0325) was detected in the diffractograms of all samples.

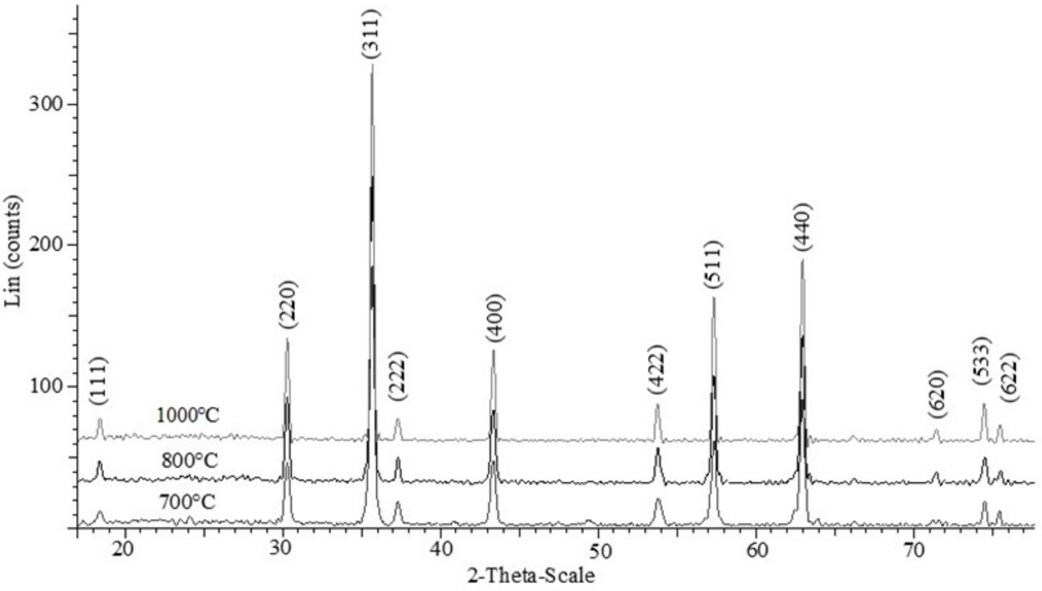

FIG. 2. Diffractograms of $NiFe_2O_4$ samples, obtained by the co-precipitation method after annealing at 700, 800 and 1000 °C for 2 h

In diffractograms of $CoFe_2O_4$ samples after annealing at 700, 800 and 1000 °C (Fig. 3), peaks corresponding to only one phase – $CoFe_2O_4$ with a cubic structure belonging to the spatial Fd3m group (JCPDS 00-022-1086) were also present.

Later, in accordance with the XPA data of MFe_2O_4 samples (M = Ni, Co), the following annealing modes were selected for the formation of $Ni_{1-x}Co_xFe_2O_4$ (x = 0.2, 0.4, 0.6 and 0.8): temperature 800 and 1000 °C, time – 2 h.

X-ray phase analysis (Figs. 4, 5) of the synthesized nanopowders demonstrated the formation of solid solutions between $NiFe_2O_4$ and $CoFe_2O_4$ [12,13], peaks with different x values coincided with each other and with standard

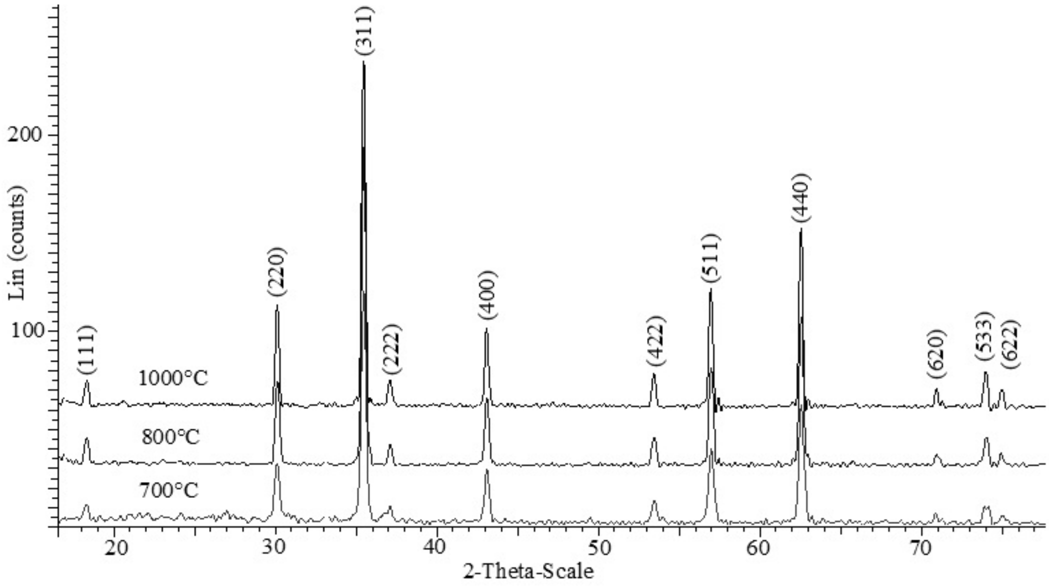

FIG. 3. Diffractograms of $CoFe_2O_4$ samples, obtained by the co-precipitation method after annealing at 700, 800 and 1000 °C for 2 h

diffractograms of JCPDS base. However, the slow scanning of the peak angles with the highest intensity (2θ was from 34.5 to 35.5 deg., Miller's indices (311)) (Fig. 4) showed the shift of X-ray diffraction lines to the left (decrease of 2θ) as x values increased (Fig. 5). This fact proves the substitution of nickel by cobalt in $Ni_{1-x}Co_xFe_2O_4$ spinel [14]. The average size of crystals of $Ni_{1-x}Co_xFe_2O_4$ spinel after annealing at 800 and 1000 °C for 2 h, calculated by formula (1), was from 19 to 50 nm and it gradually increased with an increase in the degree of doping from $x = 0$ to $x = 0.6$, and then decreased. The parameter of the crystalline cubic lattice (a) of $Ni_{1-x}Co_xFe_2O_4$ nanocrystals, calculated from formula (2), increased with increased annealing temperatures and cobalt content in the samples (Tables 1 and 2). The last trend can be explained by the fact that the ionic radius of Ni^{2+} (0.72 Å) is lower than that of Co^{2+} (0.74 Å) [11]. Similar results were obtained in studies [11, 12, 14].

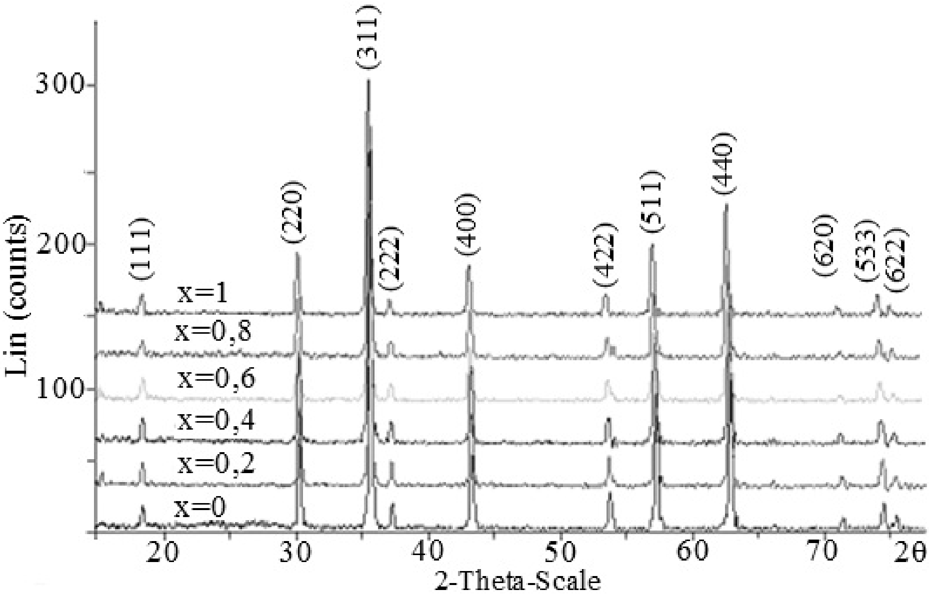

FIG. 4. Diffractograms of $Ni_{1-x}Co_xFe_2O_4$ samples obtained by the co-precipitation method after annealing at 1000 °C for 2 h

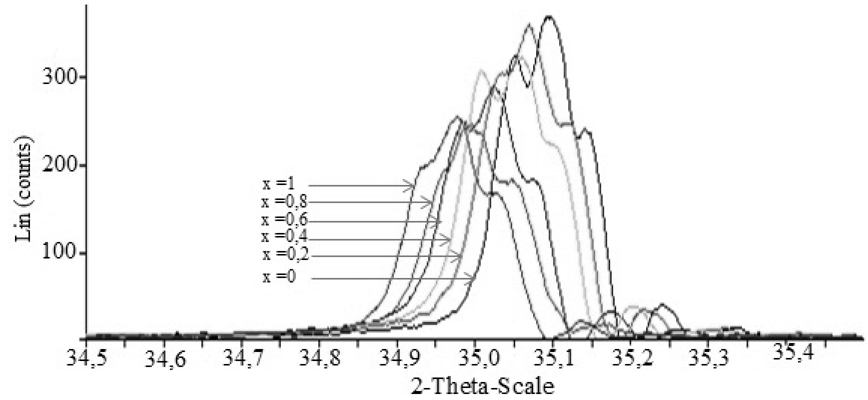

FIG. 5. Displacement of X-ray diffraction lines of $Ni_{1-x}Co_xFe_2O_4$ samples after annealing at 1000 °C for 2 h

TABLE 1. Parameters of crystalline structure of $Ni_{1-x}Co_xFe_2O_4$ samples, synthesized by the co-precipitation method after annealing at 800 °C for 2 h

x	0	0.2	0.4	0.6	0.8	1
$2\theta_{\max}$, deg	35.6714	35.6293	35.5707	35.5636	35.5244	35.4663
FWHM, rad.	0.311	0.276	0.223	0.192	0.378	0.432
D, nm	26.540	33.202	38.195	42.969	22.187	19.092
a, Å	8.311	8.351	8.364	8.366	8.375	8.387

TABLE 2. Parameters of crystalline structure of $Ni_{1-x}Co_xFe_2O_4$ samples synthesized by the co-precipitation method after annealing at 1000 °C for 2 h

x	0	0.2	0.4	0.6	0.8	1
$2\theta_{\max}$, deg	35.6756	35.6058	35.5881	35.5292	35.4835	35.4499
FWHM, rad.	0.251	0.221	0.195	0.168	0.314	0.382
D, nm	32.880	39.139	42.311	49.113	26.204	21.590
a, Å	8.340	8.356	8.366	8.373	8.384	8.392

TEM images of $NiFe_2O_4$, $Ni_{0.6}Co_{0.4}Fe_2O_4$ and $CoFe_2O_4$ samples after annealing at 800 °C for 2 h (Fig. 6) showed that the size of the synthesized particles was 30–50 nm.

The magnetization curves of $Ni_{1-x}Co_xFe_2O_4$ samples, measured at room temperature are shown in Fig. 7, while their magnetic characteristics are shown in Table 3. Analysis of the obtained results shows that saturation magnetization (M_s), excess magnetization (M_r), and coercive force (H_c) of $Ni_{1-x}Co_xFe_2O_4$ samples increase with increased cobalt content in $NiFe_2O_4$ lattice. The increase in M_r and H_c values was due to an increase in the size of $Ni_{1-x}Co_xFe_2O_4$ crystals as the cobalt content increased (see Table 2). The increase in saturation magnetization (M_s) is explained by the fact that the magnetic moment of Co^{2+} cation ($\mu = 3\mu_B$) is higher than the magnetic moment of Ni^{2+}ion ($\mu = 2\mu_B$) [17].

Excess magnetization values of the samples (M_r = 7.58–38.45 emu/g) obtained in this study were not different from data published earlier [10–12], but coercive force value (H_c = 51.94–838.42 Oe) decreased 2–3-fold depending on the value of x. The saturation magnetization (M_s = 50.3–80.45 emu/g) was not only higher than the saturation magnetization of $CoFe_2O_4$ spinel, but also much higher than the saturation magnetization of $NiFe_2O_4$ spinel [3, 4, 10, 17]. In addition, the saturation magnetization value of $CoFe_2O_4$ nanocrystals synthesized in this study, after annealing at 1000 °C for 2 h (M_s = 80.45 emu/g) was higher than the standard saturation magnetization value of $CoFe_2O_4$ multidimensional materials (M_s = 80 emu/g) [18].

Thus, $Ni_{1-x}Co_xFe_2O_4$ nanocrystals, synthesized by simple co-precipitation method, take precedence over $CoFe_2O_4$ nanocrystals by H_c value and over $NiFe_2O_4$ – by the value of M_s.

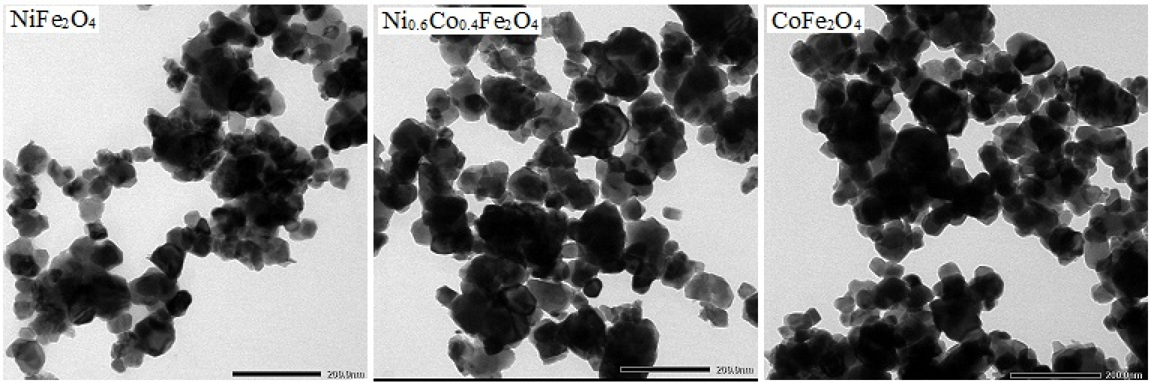

FIG. 6. TEM-images of $Ni_{1-x}Co_xFe_2O_4$ powders after annealing at 800 °C during 2 h

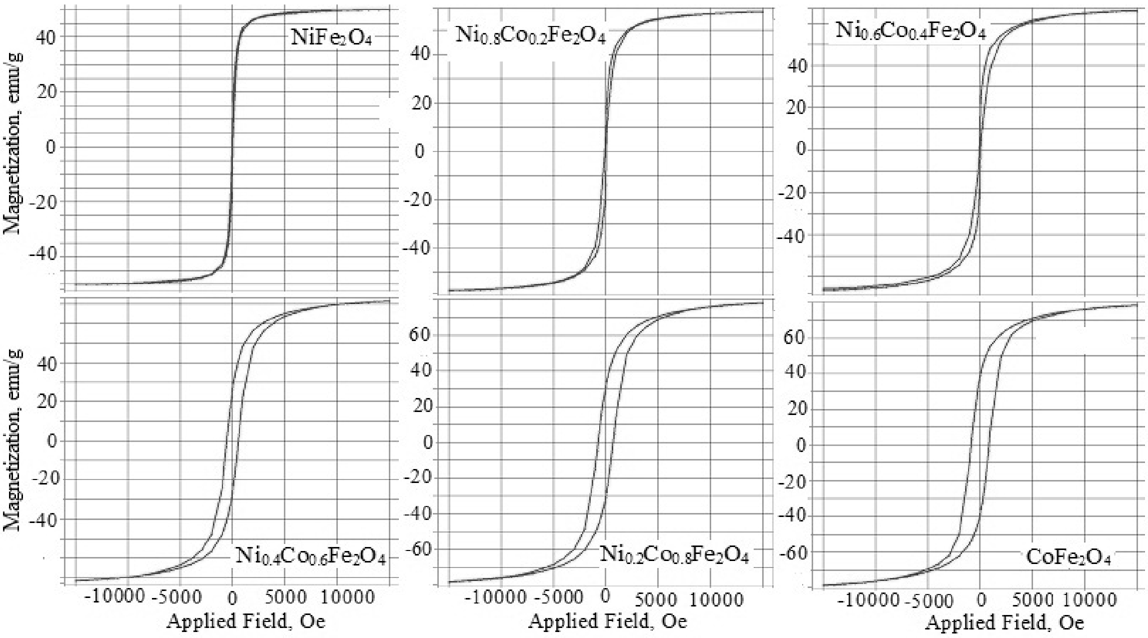

FIG. 7. Field dependence of magnetization of $Ni_{1-x}Co_xFe_2O_4$, nanocrystals synthesized by the co-precipitation method after annealing at 1000 °C for 2 h

TABLE 3. Magnetic characteristics of $Ni_{1-x}Co_xFe_2O_4$ nanocrystals synthesized by the co-precipitation method after annealing at 1000 °C for 2 h

$Ni_{1-x}Co_xFe_2O_4$	M_s, emu/g	M_r, emu/g	H_c, Oe
$x = 0$	50.3	7.58	51.94
$x = 0.2$	57.57	9.93	70.49
$x = 0.4$	66.07	10.26	73.41
$x = 0.6$	71.44	26.41	547.89
$x = 0.8$	78.16	30.96	706.26
$x = 1$	80.45	38.45	848.32

3. Conclusions

$\mathrm{Ni}_{1-x}\mathrm{Co}_x\mathrm{Fe}_2\mathrm{O}_4$ nanopowders ($x = 0$; 0.2; 0.4; 0.6; 0.8; 1) with a spinel structure were synthesized by a simple co-precipitation method using a 3 % aqueous solution of KOH as a precipitant. Single-phase samples were formed by annealing the precipitates at 700, 800 and 1000 °C for 2 h. The obtained $\mathrm{Ni}_{1-x}\mathrm{Co}_x\mathrm{Fe}_2\mathrm{O}_4$ nanocrystals had a particle size of about 30–50 nm. The size of their crystals, the cubic lattice, and the magnetic characteristics (H_c, M_r and M_s) increased with the increase of cobalt content in $\mathrm{NiFe}_2\mathrm{O}_4$ spinel.

References

[1] Ashiq M.N., Saleem S., Malana M.A., Anis R. Physical, electrical and magnetic properties of nanocrystalline Zn-Ni doped Mn-ferrite synthesized by the co-precipitation method. *Journal of Alloys and Compounds*, 2009, **486**, P. 640–644.

[2] Singhal S., Chandra K. Cation distribution and magnetic properties in chromium-substituted nickel ferrites prepared using aerosol route. *Journal of Solid State Chemistry*, 2007, **180**, P. 296–300.

[3] Seyyed Ebrahimi S.A., Azadmanjiri J. Evaluation of $\mathrm{NiFe}_2\mathrm{O}_4$ ferrite nanocrystalline powder synthesized by a sol-gel auto-combustion method. *Journal of Non-Crystalline Solids*, 2007, **353**, P. 802–804.

[4] Al Angari Y.M. Magnetic properties of La-substituted $\mathrm{NiFe}_2\mathrm{O}_4$ via egg-white precursor route. *Journal of Magnetism and Magnetic Materials*, 2011, **323**, P. 1835–1839.

[5] Nguyen A.T., Phan Ph.H.Nh., Mittova I.Ya., Knurova M.V., Mittova V.O. The characterization of nanosized $\mathrm{ZnFe}_2\mathrm{O}_4$ material prepared by coprecipitation. *Nanosystems: Physics, Chemistry, Mathematics*, 2016, **7**(3), P. 459–463.

[6] Karthick R., Ramachandran K., Srinivasan R. Study of Faraday effect on $\mathrm{Co}_{1-x}\mathrm{Zn}_x\mathrm{Fe}_2\mathrm{O}_4$ nanoferrofluids. *Nanosystems: Physics, Chemistry, Mathematics*, 2016, **7**(4), P. 624–628.

[7] Lomanova N.A., Gusarov V.V. Influence of synthesis temperature on BiFeO_3 nanoparticles formation. *Nanosystems: Physics, Chemistry, Mathematics*, 2013, **4**(5), P. 696–705.

[8] Kuznetsova V.A., Almjasheva O.V., Gusarov V.V. Influence of microwave and ultrasonic treatment on the formation of $\mathrm{CoFe}_2\mathrm{O}_4$ under hydrothermal conditions. *Glass Physics and Chemistry*, 2009, **35**(2), P. 205–209.

[9] Almjasheva O.V., Gusarov V.V. Prenucleation formations in control over synthesis of $\mathrm{CoFe}_2\mathrm{O}_4$ nanocrystalline powders. *Russian Journal of Applied Chemistry*, 2016, **89**(6), P. 851–856.

[10] Gabal M.A., Ata-Allah S.S. Effect of diamagnetic substitution on the structural. Electrical and magnetic properties of $\mathrm{CoFe}_2\mathrm{O}_4$. *Materials Chemistry and Physics*, 2004, **85**, P. 104–112.

[11] He H.-Y. Structural and magnetic property of $\mathrm{Co}_{1-x}\mathrm{Ni}_x\mathrm{Fe}_2\mathrm{O}_4$ nanoparticles synthesized by hydrothermal method. *International J. of Applied Ceramic Technology*, 2014, **11**, P. 626–636.

[12] Maaz K., Khalid W., Mumtaz A., Hasanain S.K., Liu J., Duan J.L. Magnetic characterization of $\mathrm{Co}_{1-x}\mathrm{Ni}_x\mathrm{Fe}_2\mathrm{O}_4$ nanoparticles prepared by co-precipitation route. *Physical E: Low-dimensional Systems and Nanostructures*, 2009, **41**, P. 593–599.

[13] Girgis E., Wahsh M. M.S., Othman A.G.M., Bandhu L., Rao. K.V. Synthesis. Magnetic and optical properties of core/shell $\mathrm{Co}_{1-x}\mathrm{Zn}_x\mathrm{Fe}_2\mathrm{O}_4/\mathrm{SiO}_2$ nanoparticles. *Nanoscale Res Lett*, 2011, **6**, P. 460–464.

[14] Maaz K., Karim S., Mashiatullah A., Liu J., Hou M.D., Sun Y.M., Duan J.L., Yao H.J., Mo D., Chen Y.F. Structural analysis of nickel doped cobalt ferrite nanoparticles prepared by coprecipitation route. *Physica B: Condensed Matter*, 2009, **404**, P. 3947–3951.

[15] Nguyen Anh Tien, Mittova I.Ya., Almjasheva O.V., Kirillova S.A., Gusarov V.V. Influence of the preparation condition on the size and morphology of nanocrystalline lanthanum orthoferrite. *Glass Physics and Chemistry*, 2008, **34**(6), P. 756–761.

[16] Nguyen Anh Tien, Mittova I.Ya., Almjasheva O.V. Influence of the synthesis conditions on the particle size and morphology of yttrium orthoferrite obtained from aqueous solutions. *Russian Journal of Applied Chemistry*, 2009, **82**(11), P. 1915–1918.

[17] Kubickova S., Vejpravova J., Holec P., Niznansky D. Correlation of crystal structure and magnetic properties of $\mathrm{Co}_{1-x}\mathrm{Ni}_x\mathrm{Fe}_2\mathrm{O}_4$ nanocomposites. *Journal of Magnetism and Magnetic materials*, 2013, **334**, P. 102–106.

[18] Zalite I., Heidemane G., Kodols M., Grabis J., Maiorov M. The synthesis, characterization and sintering of nickel and cobalt ferrite nanopowders. *Materials Science*, 2012, **18**(1), P. 120–124.